

Article

Enhanced Gastric/Lung Arsenic Bioaccessibility from Lignite Fly Ashes: Comparing Bioaccessibility Rates with Multiple Environmental Matrices

Anna Bourliva ^{1,*}, Efstratios Kelepertzis ², Lamprini Papadopoulou ³ , Carla Patinha ⁴ 
and Nikolaos Kantiranis ³ 

- ¹ Directorate of Secondary Education of Western Thessaloniki, 56430 Thessaloniki, Greece
² Department of Geology and Geoenvironment, National and Kapodistrian University of Athens, Panepistimiopolis, Zographou, 15784 Athens, Greece; kelepert@geol.uoa.gr
³ Department of Mineralogy-Petrology-Economic Geology, School of Geology, Aristotle University of Thessaloniki, 54124 Thessaloniki, Greece; lambrini@geo.auth.gr (L.P.); kantira@geo.auth.gr (N.K.)
⁴ GEOBIOTEC, Department of Geoscience, University of Aveiro, Campus de Santiago, 3810-193 Aveiro, Portugal; cpatinha@ua.pt
* Correspondence: annab@geo.auth.gr

Abstract: Inorganic arsenic (As), a carcinogenic element to humans, is among the most dangerous and flammable substances that coal-burning plants could release. When coal is burned, large portions of arsenic are captured on fly-ash (FA) particles, but it could also contribute significantly to stack emissions of fine fly-ash particles. The aim of this study was to evaluate the oral and respiratory bioaccessibility of arsenic in lignite fly-ash (LFA) samples, and their contribution to total As exposure. Arsenic bioaccessibility fractions via ingestion and inhalation showed significant differences, suggesting the presence of highly soluble As-bearing phases in the studied LFA samples. The bioaccessible As fractions (BAF%) in the simulated gastric fluids (UBM protocol, ISO 17924:2018) showed a range of 45–73%, while the pulmonary bioaccessibility rates in the simulated lung fluid (artificial lung fluid (ALF)) exhibited significantly enhanced levels ranging from 86% to 95%. The obtained arsenic bioaccessibility rates were compared with previous data for multiple environmental matrices such as soil and dust-related materials, revealing that LFA exhibited significantly higher bioaccessibility (%) for the inhalation pathway.

Keywords: lignite fly ash; arsenic; bioaccessibility; gastric; respiratory; mineralogy; Greece



Citation: Bourliva, A.; Kelepertzis, E.; Papadopoulou, L.; Patinha, C.; Kantiranis, N. Enhanced Gastric/Lung Arsenic Bioaccessibility from Lignite Fly Ashes: Comparing Bioaccessibility Rates with Multiple Environmental Matrices. *Toxics* **2023**, *11*, 358. <https://doi.org/10.3390/toxics11040358>

Academic Editor: Jeongim Park

Received: 9 March 2023

Revised: 2 April 2023

Accepted: 8 April 2023

Published: 10 April 2023



Copyright: © 2023 by the authors. Licensee MDPI, Basel, Switzerland. This article is an open access article distributed under the terms and conditions of the Creative Commons Attribution (CC BY) license (<https://creativecommons.org/licenses/by/4.0/>).

1. Introduction

Arsenic (As), a Group I human carcinogen [1], is a ubiquitously available metalloid in Earth's environment, typically occurring in +3 (arsenite) and +5 (arsenate) oxidation states in inorganic forms. The exposure to inorganic As through the consumption of contaminated food, water, and air, and occupational exposure have serious consequences for human health [2]. Arsenic enters the human body through a variety of routes, including ingestion, inhalation, and skin absorption. Both pentavalent and trivalent arsenic compounds are rapidly and extensively absorbed from the gastrointestinal tract. Trivalent compounds are more water-soluble than pentavalent arsenic compounds and are thereby more toxic [3].

Arsenic exposure is a consequence of natural or anthropogenic sources. Adult and child exposure to As, specifically via drinking water, has resulted in a variety of complications, including dermatological, reproductive, neurological, and cardiovascular effects, and pulmonary disorders [3–5]. Furthermore, As ingestion may cause circulatory and neurological complications, and carcinogenesis in a variety of organs, including the skin, bladder, kidneys, lungs, and liver [6,7].

Arsenic is among the most dangerous and flammable substances that coal-burning plants can release [8]. The high elemental contents of As in fly ash are well-documented [9–22]. A sum of 23 European FAs sourced from coal-burning power plants exhibited As contents ranging from 22 to 162 mg kg⁻¹ with an average of 55 mg kg⁻¹ [17]. Regarding Greek fly ash, Georgakopoulos et al. [10] reported As contents ranging from 20.5 to 38.8 mg kg⁻¹, while Samara [8] found As contents up to 46.9 mg kg⁻¹. Moreover, the chemical speciation of As in FA is essential and was extensively studied [23–25]. Arsenic in FAs occurs mainly as pentavalent arsenate As(V) with minor trivalent arsenite As(III), which might be associated with glass, iron (oxyhydr)oxides, and calcium arsenate.

Arsenic, in contrast to other elements, shows strong affinity to the finest fly-ash fractions [26,27]. Fly ash with smaller particles could readily pass through the body's respiratory system, enter the stomach, and float in the air. Thus, incidental ingestion and inhalation are important non-dietary As exposure pathways for both adults and children [28]. Although exposure assessment was previously based on total metal(loid) content, bioavailability (i.e., absorption in the systemic circulation) and/or bioaccessibility (i.e., solubility in simulated biological fluids)-based approach is currently dominating that offers more accurate exposure quantification. The limitations and ethical considerations of *in vivo* exposure assessment methods have led to *in vitro* bioaccessibility methods being a potential alternative that supplements data for exposure assessment [29]. As a result, information is critical on bioaccessible As fractions, i.e., soluble As fractions in the target compartment's conditions (gastrointestinal or respiratory).

The high toxicity of As, especially if one is exposed via inhalation [30,31], indicates the importance to investigate its bioaccessibility to better quantify exposure. A growing number of studies were conducted in this context to determine the bioaccessible fraction of As in particulate matter, soil, and dust [32–37]. Despite significant concerns about the health risks of As release in simulated biological fluids, there are relatively few studies on gastric/lung As bioaccessibility from fly ash. Jin et al. [38] reported that bioaccessible (gastric and intestinal) arsenic was in the range of 36–67% for Chinese fly-ash samples. Lokeshappa et al. [39] determined that more than 40% of As was in bioaccessible form via ingestion from Ca-rich and Si-rich fly ash using a physiological extraction test (PBET). The objectives of the present study are to (a) evaluate As distribution in ingestible and inhalable size fractions of Greek lignite fly ash (LFA), (b) determine bioaccessible As fractions via the ingestion and inhalation of LFA, and (c) compare the bioaccessibility rates with published data.

2. Materials and Methods

2.1. Lignite Fly-Ash Samples

We used five lignite fly-ash (LFA) samples (AD, KD, AM, MG1, MG2) produced in lignite-fired power plants operating in the main lignite basins of Greece. Details of the power plants (PPs), sample pretreatment, and the main physicochemical characteristics were presented elsewhere [40,41]. We studied Ca-rich LFA from plants operating in the Ptolemais–Amynteo (P–A) lignite basin (AD, Agios Dimitrios PP; KD, Kardias PP; AM, Amynteo PP) and Si-rich LFA from power plants operating in the Megalopolis basin (MG1 and MG2). Ingestible (<250 µm) and inhalable (<10 µm) particle size fractions were separated with dry sieving for the gastric and lung bioaccessibility tests, respectively. All samples were sealed and stored (<4 °C) until further analysis.

2.2. Analytical Methods

The mineralogical characterization of the studied LFA size fractions (<250 and <10 µm) was performed with a water-cooled Rigaku Ultima diffractometer with CuKα radiation, a step size of 0.05°, and a step time of 3 s operating at 40 kV and 30 mA. Morphological characteristics and differences among LFA particle sizes were examined with scanning electron microscopy (SEM) on a JEOL JSM-840A microscope operating at 20 kV connected with an X-ray energy dispersive spectrometer (EDX; INCA 300).

The elemental concentrations of major elements Si, Ti, Al, Fe, Mn, Mg, Ca, K, P, and S were determined via pXRF. A Bruker S1 Titan 600 with a 4 W Rh X-ray tube, 5 mm spot size, a silicon drift detector (resolution < 145 eV), and the inbuilt Geoexploration mode, a factory calibration method for soils, was used for pXRF analysis. The analysis was conducted in three energy ranges (15, 30 and 50 kV) for 30 s each (a total of 90 s). The elemental contents calculated with the Geoexploration mode were calibrated using certified reference materials (CRMs); calibration curves with R^2 values higher than 0.9 were obtained.

The near-total As contents were determined after an aqua regia digestion using inductively coupled plasma mass spectrometry (ICP–MS) at ActLabs Analytical Laboratories Ltd., Canada (for the ingestible size fraction < 250 μm) and GeoBioTec Laboratory, University of Aveiro, Portugal (for the inhalable size fraction < 10 μm). Quality assurance and quality control (QA/QC) included reagent blanks, analytical replicates, sample duplicates, and analyses of inhouse reference materials. The recovery rates were estimated within $\pm 10\%$ of the certified value, and analytical precision (expressed as RSD %) was <10%.

Both the oral and lung bioaccessibility determinations of As were carried out in GeoBioTec, University of Aveiro, Portugal. The <250 μm particle size was utilized for the oral bioaccessibility tests since this soil portion adheres to human hands and becomes ingested during hand-to-mouth activity [42]. Smaller particles, specifically the <10 μm size fraction, were selected for the lung bioaccessibility tests since they could be deposited in the tracheal–bronchial and alveolar region, thus posing the greatest risk via inhalation [29].

Oral bioaccessibility was determined using the unified bioaccessibility method (UBM) validated against an in vivo model [43]. The UBM protocol [44] is a two-stage in vitro procedure that simulates the leaching of a solid matrix in both the gastric (G) and gastrointestinal-tract (GI) phases by using synthetic digestive solutions according to physiological transit times. Specifically, the procedure consists of consecutive steps in simulated human saliva and gastric juice (G phase, 37 °C, 1 h, pH 1.2 ± 0.05), and then in simulated bile and duodenal fluid (GI phase, 37 °C, 4 h, pH 6.3 ± 0.5). The samples were shaken at 37 °C on an end-over-end shaker, and the particles were separated from the solutions with centrifugation at $4500 \times g$ for 15 min. Lung bioaccessibility determinations were performed using an artificial lysosomal fluid (ALF) solution (pH 4.5) that simulates intracellular conditions in the lungs and extracts higher concentrations of metals than those of other commonly used simulated lung fluids [45]. In brief, 0.05 g (± 0.0001) of the inhaled size fraction (<10 μm) was weighed into 85 mL polycarbonate centrifuge tubes, and 50 mL of the simulated fluid (ratio of 1:1000) was added. The samples were shaken at 37 °C on an end-over-end shaker for 24 h, and the particles were separated from the solution by centrifugation at $4500 \times g$ for 15 min. Both digestive and lung simulated biological fluids (SBFs) were freshly prepared prior to extraction. Bioaccessible oral and pulmonary As (including both As^{3+} and As^{5+}) concentrations (mg kg^{-1}) in the supernatants were prepared with ICP–MS. UBM-specific certified reference soil BGS102 (ironstone soil from Lincolnshire, UK) that provides UBM guidance values [46,47] was used in order to validate the uncertainty of the extraction protocol. For BGS102, the recovery rate for As was 115.4% for the gastric phase and 113.2% for the gastrointestinal phase. Though respiratory bioaccessibility values for several elements were reported for standard reference material BCR-723 [45], there are no reported values for arsenic.

3. Results and Discussion

3.1. Mineralogy and Morphology of LFA Size Fractions

The mineralogical composition of the bulk (<250 μm) LFA samples was discussed elsewhere [41]. Here, the mineralogical differences in the different particle sizes were further investigated, and representative XRD patterns are given in Figure 1.

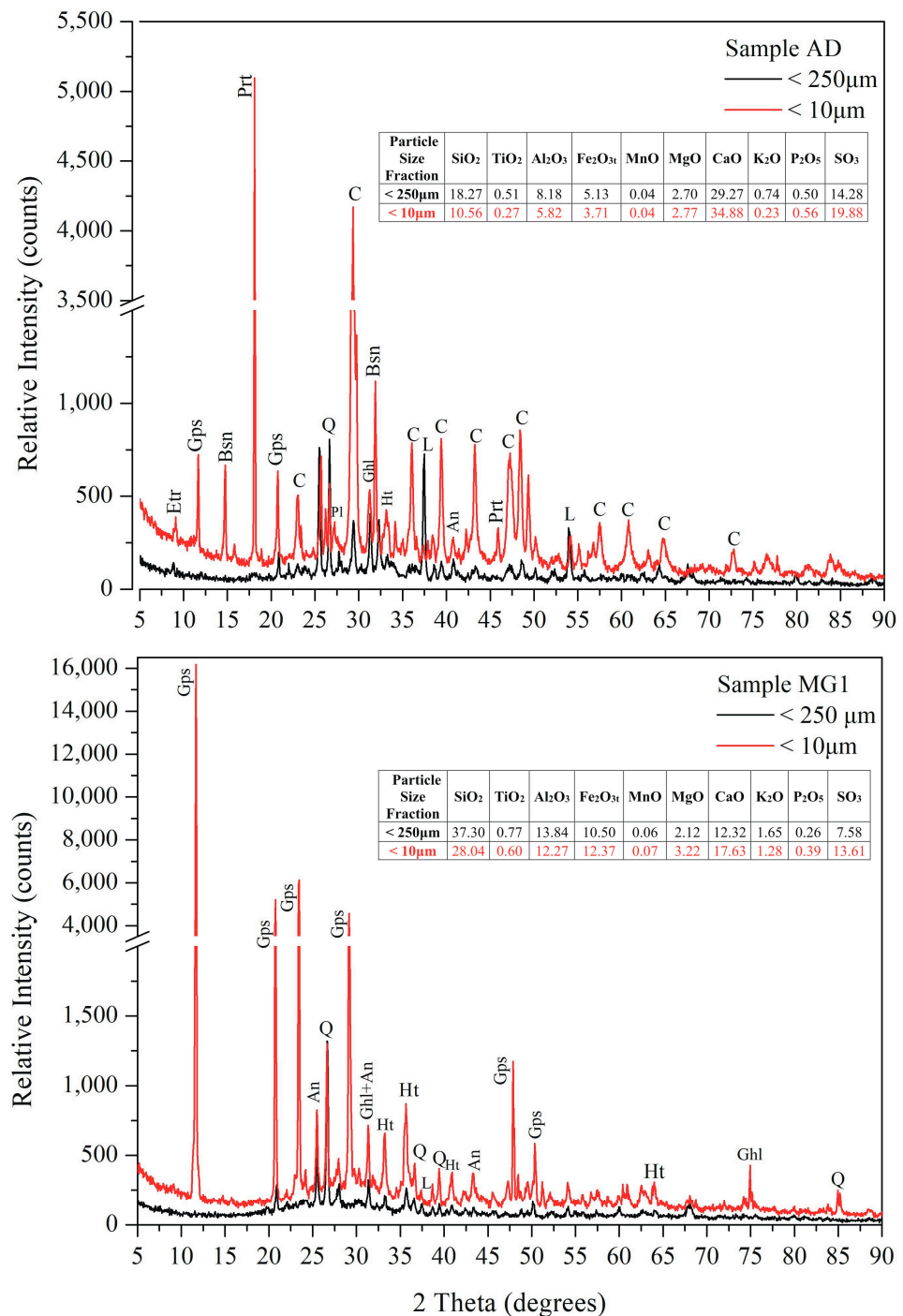


Figure 1. Representative XRD patterns of Ca-rich (Sample AD, **top**) and Si-rich (Sample MG1, **bottom**) fly-ash samples of the two different studied size fractions. An: anhydrite, Bsn: bassanite, C: calcite, Etr: ettringite, Ghl: gehlenite, Gps: gypsum, Ht: hematite, L: lime, Prt: portlandite, Pl: plagioclase, Q: quartz. The concentration units of pXRF results are given in the insets.

As reported [41], ingestible LFA fractions (<250 μm) contained both amorphous and crystalline mineral phases with quartz and a number of Ca-bearing mineral phases dominating. Significant differences in the mineralogy of the inhalable size fraction (<10 μm) of Ca- and Si-rich LFA were revealed. Specifically, quartz content decreased with the decrease in particle size, indicating that quartz tended to aggregate in the coarse fly-ash fractions. Inversely, the calcium mineral content greatly increased with the decrease in particle size, showing a relatively high content of Ca-bearing minerals in finer LFA fractions.

Specifically, Ca-rich LFA revealed high contents of secondary Ca-bearing mineral phases such as calcite (CaCO_3), Ca hydroxides (i.e., portlandite) and Ca sulphates (i.e., gypsum, bassanite) and/or Ca–Al sulphates (i.e., ettringite). Similarly, Si-rich LFA exhibited significantly higher Ca-bearing phases (i.e., gypsum, calcite), in contrast with the coarser fractions, where Si-rich minerals (i.e., quartz, feldspars) dominated. Moreover, Fe-bearing phases (i.e., hematite) tended to accumulate in the finer LFA fractions. The aforementioned findings are supported by XRF analysis in both size fractions (Figure 1, inlets).

SEM observations revealed the dominance of typical spherular fly-ash particles with sizes ranging from 1 to 100 μm , while irregular aggregates and needlelike particles (mainly Ca sulphates) were also observed (Figure 2). As already reported [41], Ca-rich LFA were dominated by irregularly shaped Si-rich particles and angular Ca-rich agglomerates in a wide range of sizes, while Si-rich LFA exhibited a plethora of Si-rich and/or Fe-rich spherules with lower contents of Ca, Al, and Mg.

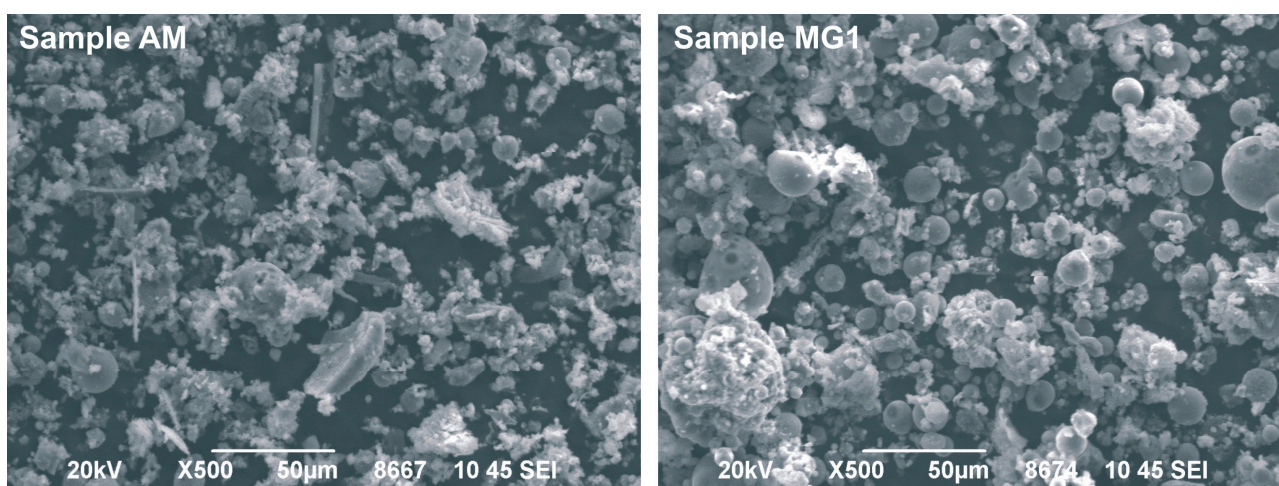


Figure 2. Representative SEM images of the studied fly-ash samples.

3.2. Arsenic Contents in LFA Size Fractions

Near-total As concentrations in the studied LFA size fractions are illustrated in Figure 3. Near-total As concentrations in the $<250 \mu\text{m}$ size fraction (total $\text{As}_{250 \mu\text{m}}$) ranged between 10 and 41 mg kg^{-1} with a mean As content of 21.2 mg kg^{-1} (Figure 3). The concentration of As in the finer fraction (total $\text{As}_{10 \mu\text{m}}$) exhibited a mean value of 69.2 mg kg^{-1} with severe variation in As content among the LFA samples from different power plants. Specifically, total $\text{As}_{10 \mu\text{m}}$ varied from 19.8 (KD) to 143.9 mg kg^{-1} (MG1). The descending order of $\text{MG1} > \text{MG2} > \text{AD} > \text{AM} > \text{KD}$ was observed, with significantly higher As contents being recorded in the Si-rich LFA (MG1 and MG2). Specifically, Si-rich LFA exhibited an average of almost 140 mg kg^{-1} of As compared to an average of 22 mg kg^{-1} in Ca-rich LFA. Moreover, a negative correlation was revealed between As concentration and particle size. As contents were increased with the decrease in particle size from 250 to 10 μm ; especially for Si-rich LFA, this increase was quite sharp. Specifically, total $\text{As}_{10 \mu\text{m}}$ was almost 3 to 7 times higher than the corresponding one in the coarser fraction ($<250 \mu\text{m}$) for MG LFA samples, and up to 2.2 times higher for the P-A LFA samples.

The findings demonstrate As enrichment in finer LFA particles and are in agreement with earlier reports [11,38]. Although a direct comparison of As contents is difficult due to the different applied analytical methods and utilized particle size fractions, the obtained As concentrations in the $<250 \mu\text{m}$ size fraction were relatively lower than those reported for European coal fly ash [17] and globally for different FA types [48–50]. However, the finer LFA fractions were significantly enriched in As, with the average within the reported ranges of arsenic for European FA (Figure 3).

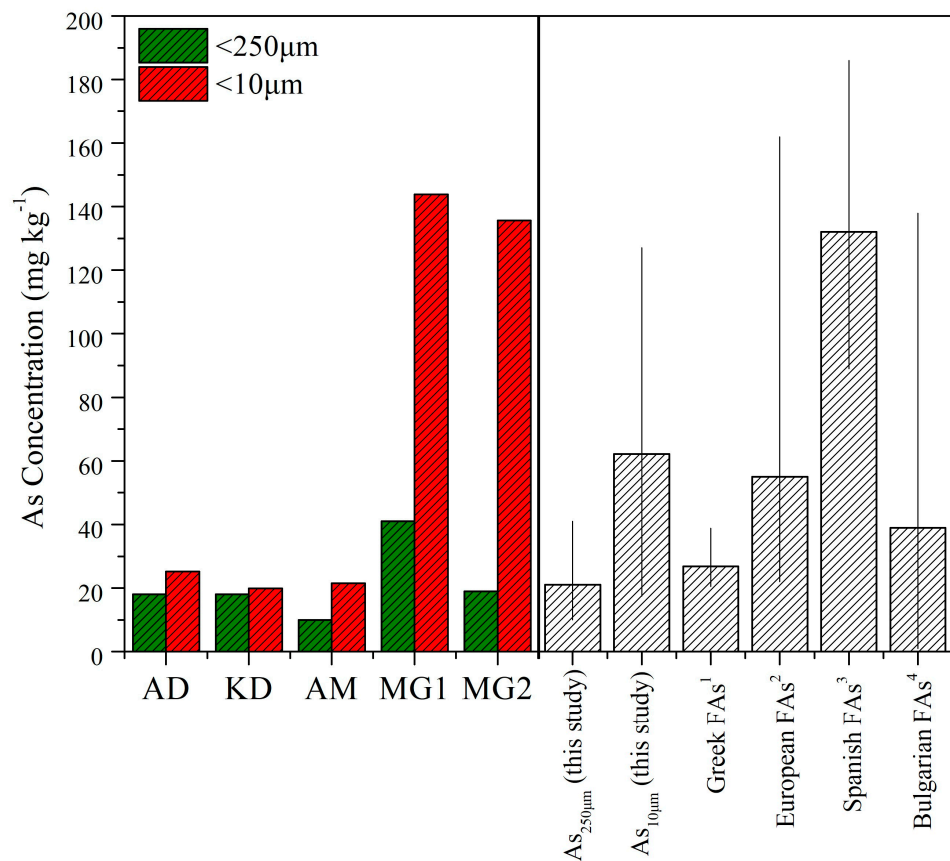


Figure 3. Arsenic concentrations (mg kg^{-1}) in the <250 and <10 μm size fractions, and a comparison of the obtained As contents with published data ¹ [10], ² [17], ³ [49], ⁴ [48].

3.3. Arsenic Gastric/Lung Bioaccessibility Data

The bioaccessible As concentrations (mg kg^{-1}) in the simulated gastric/gastrointestinal and lung fluids are presented in Figure 4.

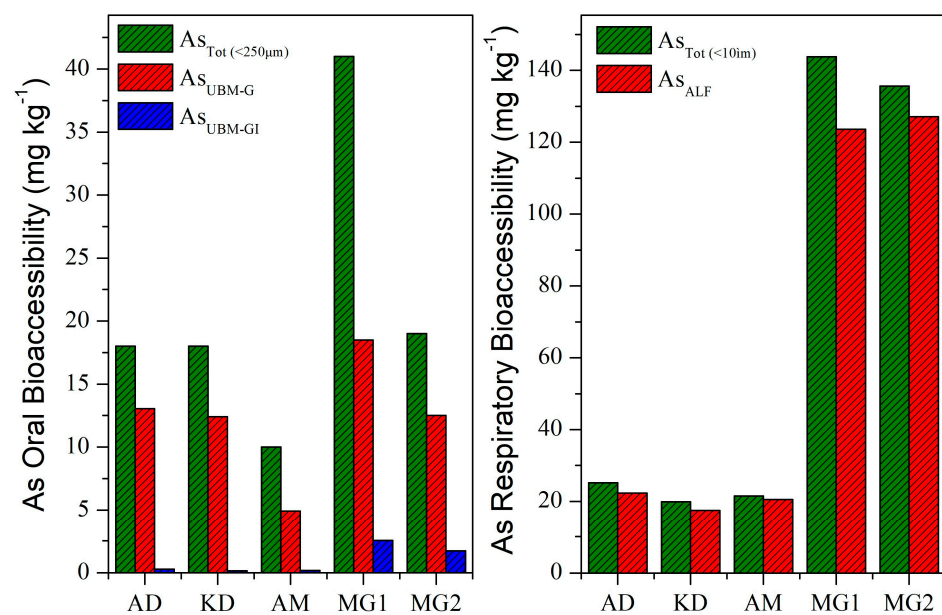


Figure 4. Arsenic bioaccessibility (in mg kg^{-1}) of lignite fly-ash samples in (left) gastric (G)/gastrointestinal (GI) and (right) lung fluids.

The UBM-extractable As contents in the gastric phase ranged from 4.9 (AM) and 18.5 mg kg⁻¹ (MG1) with an average value of 12.3 mg kg⁻¹. The UBM-extractable As concentrations (G-phase) in the studied LFA exhibited the decreasing order of MG1 > AD > MG2 > KD > AM, with a significant correlation between UBM-extractable As concentrations and total As contents ($r^2 = 0.897$). Significantly lower UBM-extractable As contents were recorded in the GI phase with the range of 0.2–2.5 mg kg⁻¹. Such a decrease in As bioaccessible contents in the simulated intestinal phase was also reported by Jin et al. [38]. These surprisingly lower bioaccessibility values are indicative of the influence of the matrix type that, in combination with parameters in the simulated GI-phase, may lead to the complexation and precipitation of As from the solution, and needs further investigation. On the other hand, ALF-extractable As contents (mean, 62.2 mg kg⁻¹) were higher than the corresponding UBM-extractable ones (mean, 12.3 mg kg⁻¹) in the gastric phase, especially for Si-rich LFA samples (Samples MG1 and MG2). The higher extractable contents in the lung fluid (ALF) indicate the aggressiveness of the method [45]. ALF-extractable As contents exhibited great variability among samples, with values ranging from 17.5 (KD) to 127.1 mg kg⁻¹ (MG2); a different descending order was recorded: MG2 > MG1 > AD > AM > KD. A strong correlation ($r^2 = 0.998$) between total and ALF-extractable As contents suggests that total As contents might be a good indicator of lung bioaccessibility.

A different trend on gastric/lung bioaccessibility was revealed when extractable As contents were expressed as percentages with respect to the total As contents (Figure 5). The bioaccessible As fractions (BAF%) via ingestion showed the range of 45.1–72.5%. The descending order of AD > KD > MG2 > AM > MG1 was recorded, indicating that As was relatively more bioaccessible in the Ca-rich LFA, which was in line with our previous study concerning multiple trace elements [41]. Significantly higher bioaccessible As fractions were recorded in the artificial lung fluid ranging between 86% (AD) and 95% (MG2). Despite the differences in total As_{10 μm} contents from the five plants, the bioaccessible As fractions via inhalation were similar, suggesting the presence of highly soluble As-bearing phases in all samples.

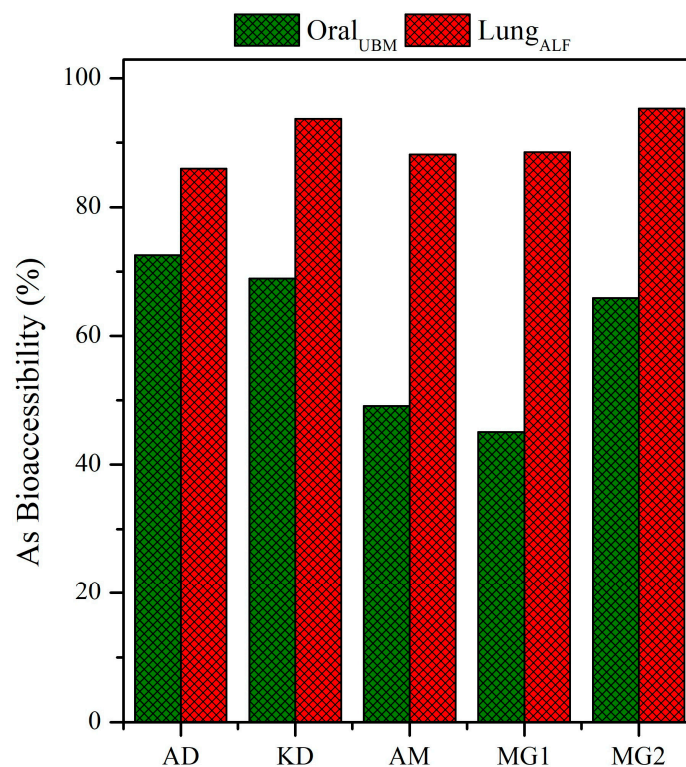


Figure 5. Arsenic bioaccessibility (%) of lignite fly-ash samples in gastric and lung fluids.

lower bioaccessible concentrations of As in the surface soil ($3.4 \pm 2\%$) and residential FSD samples ($2.7 \pm 1\%$).

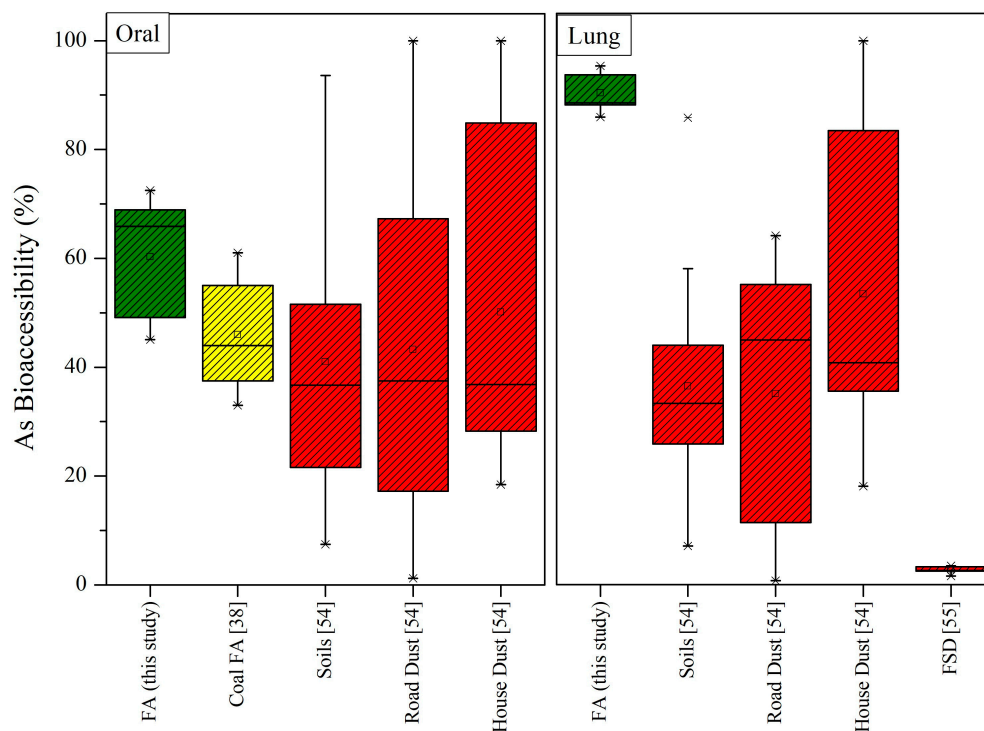


Figure 7. Comparison of As bioaccessible fractions (%) between LFA and other environmental materials. Data for other coal FAs are from Jin et al. [38], for soil, road dust, and house dust are from Kelepertzis et al. [54], and those for fine surface dust (FSD) are from Morais et al. [55]. The box is determined by the 25th and 75th percentiles. The whiskers (—) are determined by the 5th and 95th percentiles. Additionally, the minimum (*), median (line), mean (□) and maximum (*) values are presented. Green boxes: this study; Yellow boxes: other FAs; Red boxes: other materials.

The above indicate that both gastric and lung bioaccessible As fractions (%) showed great variation among the compared matrices. Specifically, for the ingestion pathway, As bioaccessibility followed the order of LFA > house dust ≥ road dust > soil; for the inhalation pathway, the order was similar, namely, LFA > house dust > soil ≥ road dust > FSD, suggesting the presence of highly soluble As-bearing phases in the studied LFA samples. Interestingly, the differences in BAF (%) between the LFAs and the other environmental media were more pronounced for respiratory bioaccessibility. The overall comparison of the BAFs of As in the studied LFAs with data from several authors for a variety of environmental sampling media clearly demonstrate the significantly higher As bioaccessibility in LFA, especially for the inhalation pathway. of the sources of variability are probably related to the physicochemical factors of the samples (sample type, particle size, speciation) or even the protocol parameters (extraction time, solid/liquid ratio, temperature, and agitation). For instance, the inhalation bioaccessibility results on the applied SLF presented by Kelepertzis et al. [54] were on a coarser size fraction (<100 μm) for which the rate and extent of As dissolution was probably diminished; consequently, lower As bioaccessibility results were potentially obtained. Moreover, variation in the bioaccessibility rates indicates that the simulated lung fluids “attacked” either different As-containing phases or identical phases with varying intensity. The importance of metal(loid) speciation in influencing bioaccessibility was also extensively reported [51,53].

4. Conclusions

In this study, As contents and bioaccessible fractions in ingestible (<250 µm) and inhalable (<10 µm) size fractions of Greek lignite fly ash (LFA) were evaluated. Lignite fly-ash samples of different chemical types (i.e., Ca-rich and Si-rich) were from coal-fired power plants operating in the main lignite basins of Greece. Differences in the mineralogical composition of the studied size fractions were revealed. Specifically, quartz exhibited increased contents in the coarser LFA fractions (<250 µm), while Ca-bearing mineral phases were relatively enriched in the finer LFA fractions. Arsenic contents in the ingestible size fraction (total As_{250 µm}) exhibited the range of 10–41 mg kg⁻¹, while significantly higher concentrations were recorded in the inhalable LFA fraction (total As_{10 µm}) ranging from 19.8 mg kg⁻¹ (Ca-rich LFA sample) to 143.9 mg kg⁻¹ (Si-rich LFA sample), indicating an As enrichment character in fine fractions that should raise public concern. Gastric As bioaccessible fractions ranged from 45.1% to 72.5%, while 86–95% of As was bioaccessible via the inhalation pathway. Though the comparison of bioaccessibility rates should be treated with caution, Greek lignite fly ash demonstrates substantial higher bioaccessibility rates, especially via the inhalation pathway, indicating that the investigated LFA samples contained highly soluble As-bearing phases, which is highly concerning. These findings highlight the significance of characterizing the bioaccessibility rates of LFA in health risk assessment, and this may help in guiding ongoing efforts to reduce public health risk.

Author Contributions: Conceptualization, A.B.; formal analysis, L.P., C.P. and N.K.; investigation, A.B.; data curation, A.B. and E.K.; writing—original draft preparation, A.B. and E.K.; writing—review and editing, A.B., E.K., L.P., C.P. and N.K. All authors have read and agreed to the published version of the manuscript.

Funding: This research received no external funding.

Data Availability Statement: The presented data in this study are contained within the article.

Acknowledgments: The authors would like to thank Eduardo Ferreira da Silva for allowance of performing the bioaccessibility tests in the GeoBioSciences, Geotechnologies, and Geoenvironment (GEOBIOTEC) research unit, Department of Geoscience, University of Aveiro. Finally, the authors would like to thank three anonymous reviewers for their comments and suggestions.

Conflicts of Interest: The authors declare no conflict of interest.

References

1. IARC (International Agency for Research on Cancer). *Arsenic, Metals, Fibres, and Dusts. Monographs on the Evaluation of Carcinogenic Risks to Humans. A Review of Human Carcinogens*; IARC (International Agency for Research on Cancer): Lyon, France, 2012; Volume 100 (C).
2. Henke, K. *Arsenic: Environmental Chemistry, Health Threats and Waste Treatment*; John Wiley & Sons Ltd.: Chichester, UK, 2009; pp. 69–235.
3. Mohammed Abdul, K.S.; Jayasinghe, S.S.; Chandana, E.P.S.; Jayasumana, C.; De Silva, P.M. Arsenic and human health effects: A review. *Environ. Toxicol. Pharmacol.* **2015**, *40*, 828–846. [[CrossRef](#)] [[PubMed](#)]
4. Dauphiné, D.C.; Smith, A.H.; Yuan, Y.; Balmes, J.R.; Bates, M.N.; Steinmaus, C. Case-control study of arsenic in drinking water and lung cancer in California and Nevada. *Int. J. Environ. Res. Public Health* **2013**, *10*, 3310–3324. [[CrossRef](#)] [[PubMed](#)]
5. Sohel, N.; Vahter, M.; Ali, M.; Rahman, M.; Streatfield, P.K.; Kanaroglou, P.S.; Persson, L.A. Spatial patterns of fetal loss and infant death in an arsenic-affected area in Bangladesh. *Int. J. Health Geogr.* **2010**, *9*, 53. [[CrossRef](#)] [[PubMed](#)]
6. Celik, I.; Gallicchio, L.; Boyd, K.; Lam, T.K.; Matanoski, G.; Tao, X.G.; Shiels, M.; Hammond, E.; Chen, L.W.; Robinson, K.A.; et al. Arsenic in drinking water and lung cancer: A systematic review. *Environ. Res.* **2008**, *108*, 48–55. [[CrossRef](#)]
7. Smith, A.H.; Goycolea, M.; Haque, R.; Biggs, M.L. Marked increase in bladder and lung cancer mortality in a region of Northern Chile due to arsenic in drinking water. *Am. J. Epidemiol.* **1998**, *7*, 660–669. [[CrossRef](#)]
8. Shen, Y.-W.; Zhao, H.; Xie, J.-J.; He, K.-Q.; Pang, J.-F.; Guo, Q.; Duan, X.-L.; Yuan, C.-G.; Zhang, K.-G.; Zhu, H.-T.; et al. Insight of the size dependent bioavailability and health risk assessment of arsenic in resuspended fly ash from power plants. *Fuel* **2022**, *327*, 125049. [[CrossRef](#)]
9. Dai, S.; Ren, D.; Chou, C.L.; Finkelman, R.B.; Seredin, V.V.; Zhou, Y.P. Geochemistry of trace elements in Chinese coals: A review of abundances, genetic types, impacts on human health, and industrial utilization. *Int. J. Coal Geol.* **2011**, *94*, 3–21. [[CrossRef](#)]
10. Georgakopoulos, A.; Filippidis, A.; Kassoli-Fournaraki, A.; Iordanidis, A.; Fernandez-Turiel, J.F.L.; Gimeno, D. Environmentally important elements in fly ashes and their leachates of the power stations of Greece. *Energy Sources* **2002**, *24*, 83–91. [[CrossRef](#)]

11. Gong, B.; Yong, Q.; Xiong, Z.; Tian, C.; Yang, J.; Zhao, Y.; Zhang, J. Mineral matter and trace elements in ashes from a high-arsenic lignite fired power plant in Inner Mongolia, China. *Int. J. Coal Geol.* **2018**, *196*, 317–334. [[CrossRef](#)]
12. Han, D.; Xu, L.; Wu, Q.; Wang, S.; Duan, L.; Wen, M.; Li, Z.; Tang, Y.; Li, G.; Liu, K. Potential environmental risk of trace elements in fly ash and gypsum from ultra-low emission coal-fired power plants in China. *Sci. Total Environ.* **2021**, *798*, 149116. [[CrossRef](#)]
13. Kostova, I.; Vassileva, C.; Dai, S.; Hower, J.C. Mineralogy, geochemistry and mercury content characterization of fly ashes from the Maritza 3 and Varna thermoelectric power plants, Bulgaria. *Fuel* **2016**, *186*, 674–684. [[CrossRef](#)]
14. Koukouzas, N.K.; Zeng, R.; Perdikatsis, V.; Xu, W.; Kakaras, E. Mineralogy and geochemistry of Greek and Chinese coal fly ash. *Fuel* **2006**, *85*, 2301–2309. [[CrossRef](#)]
15. Medina, A.; Gamero, P.; Querol, X.; Moreno, N.; DeLeón, B.; Almanza, M. Fly ash from a Mexican mineral coal I: Mineralogical and chemical characterization. *J. Hazard. Mater.* **2010**, *181*, 82–90. [[CrossRef](#)] [[PubMed](#)]
16. Meij, R.; Winkel, B.H. Trace elements in world steam coal and their behavior in Dutch coal-fired power stations: A review. *Int. J. Coal Geol.* **2009**, *77*, 289–293. [[CrossRef](#)]
17. Moreno, N.; Querol, X.; Andrés, L.M.; Stanton, K.; Towler, M.; Nugteren, H.; Janssen-Jurkovicová, M.; Jones, R. Physico-chemical characteristics of European pulverized coal combustion fly ashes. *Fuel* **2005**, *84*, 1351–1363. [[CrossRef](#)]
18. Samara, C. Chemical mass balance source apportionment of TSP in a lignite-burning area of Western Macedonia, Greece. *Atmos. Environ.* **2005**, *39*, 6430–6443. [[CrossRef](#)]
19. Tian, H.Z.; Lu, L.; Hao, J.M.; Gao, J.J.; Cheng, K.; Liu, K.Y.; Qiu, P.P.; Zhu, C.Y. A review of key hazardous trace elements in Chinese coals: Abundance, occurrence, behavior during coal combustion and their environmental impacts. *Energy Fuels* **2013**, *27*, 601–614. [[CrossRef](#)]
20. Vassilev, S.; Vassileva, C. Mineralogy of combustion wastes from coal-fired power stations. *Fuel Process. Technol.* **1996**, *47*, 261–280. [[CrossRef](#)]
21. Zhang, Y.; Shang, P.; Wang, J.; Norris, P.; Romero, C.E.; Pan, W.-P. Trace element (Hg, As, Cr, Cd, Pb) distribution and speciation in coal-fired power plants. *Fuel* **2017**, *208*, 647–654. [[CrossRef](#)]
22. Zhao, S.; Duan, Y.; Lu, J.; Gupta, R.; Pudasainee, D.; Liu, S.; Liu, M.; Lu, J. Chemical speciation and leaching characteristics of hazardous trace elements in coal and fly ash from coal-fired power plants. *Fuel* **2018**, *232*, 463–469. [[CrossRef](#)]
23. Fu, B.; Hower, J.C.; Dai, S.; Mardon, S.M.; Liu, G. Determination of Chemical Speciation of Arsenic and Selenium in High-As Coal Combustion Ash by X-ray Photoelectron Spectroscopy: Examples from a Kentucky Stoker Ash. *ACS Omega* **2018**, *3*, 17637–17645. [[CrossRef](#)] [[PubMed](#)]
24. Itaya, Y.; Kuninishi, K.; Hashimoto, Y. Arsenic, selenium, and chromium speciation in fly ash. *J. Mater. Cycles Waste Manag.* **2022**, *24*, 250–258. [[CrossRef](#)]
25. Tian, C.; Hu, Y.; Tian, X.; Huang, Z. Deep insights on arsenic speciation and partition in coal-fired particles from micro to nano size. *Fuel* **2023**, *332*, 126159. [[CrossRef](#)]
26. Ronkkumäki, H.; Poykio, R.; Nurmesniemi, H.; Popov, K.; Merisalu, E.; Tuomi, T.; Valimäki, L. Particle size distribution and dissolution properties of metals in cyclone fly ash. *J. Environ. Sci. Technol.* **2008**, *5*, 485–494.
27. Zielinski, R.A.; Foster, A.L.; Meeker, G.P.; Brownfield, I.K. Mode of occurrence of arsenic in feed coal and its derivative fly ash, Black Warrior Basin, Alabama. *Fuel* **2007**, *86*, 560–572. [[CrossRef](#)]
28. ATSDR. *Public Health Statement for Arsenic*; Agency for Toxic Substances and Disease Registry, Division of Toxicology and Environmental Medicine: Atlanta, Georgia, 2007.
29. Kastury, F.; Smith, E.; Juhasz, A.L. A critical review of approaches and limitations of inhalation bioavailability and bioaccessibility of metal(loid)s from ambient particulate matter or dust. *Sci. Total Environ.* **2017**, *574*, 1054–1074. [[CrossRef](#)]
30. Guney, M.; Chapuis, R.P.; Zagury, G.J. Lung bioaccessibility of contaminants in particulate matter of geological origin. *Environ. Sci. Pollut. Res.* **2016**, *23*, 24422–24434. [[CrossRef](#)]
31. Yager, J.W.; Greene, T.; Schoof, R.A. Arsenic relative bioavailability from diet and airborne exposures: Implications for risk assessment. *Sci. Total Environ.* **2015**, *536*, 368–381. [[CrossRef](#)]
32. Drahotová, P.; Raus, K.; Rychlíková, E.; Rohovec, J. Bioaccessibility of As, Cu, Pb, and Zn in mine waste, urban soil, and road dust in the historical mining village of Kaňk, Czech Republic. *Environ. Geochem. Health* **2018**, *40*, 1495–1512. [[CrossRef](#)]
33. Huang, M.; Chen, X.; Zhao, Y.; Chan, C.Y.; Wang, W.; Wang, X.; Wong, M.H. Arsenic speciation in total contents and bioaccessible fractions in atmospheric particles related to human intakes. *Environ. Pollut.* **2014**, *188*, 37–44. [[CrossRef](#)]
34. Kim, E.J.; Yoo, J.-C.; Baek, K. Arsenic speciation and bioaccessibility in arsenic-contaminated soils: Sequential extraction and mineralogical investigation. *Environ. Pollut.* **2014**, *186*, 29–35. [[CrossRef](#)] [[PubMed](#)]
35. Liu, Y.; Ma, J.; Yan, H.; Ren, Y.; Wang, B.; Lin, C.; Liu, X. Bioaccessibility and health risk assessment of arsenic in soil and indoor dust in rural and urban areas of Hubei province, China. *Ecotoxicol. Environ. Saf.* **2016**, *126*, 14–22. [[CrossRef](#)] [[PubMed](#)]
36. Martin, R.; Dowling, K.; Nankervis, S.; Pearce, D.; Florentine, S.; McKnight, S. In vitro assessment of arsenic mobility in historical mine waste dust using simulated lung fluid. *Environ. Geochem. Health* **2018**, *40*, 1037–1049. [[CrossRef](#)] [[PubMed](#)]
37. Wiseman, C.L.S.; Zereini, F. Characterizing metal(loid) solubility in airborne PM₁₀, PM_{2.5} and PM₁ in Frankfurt, Germany using simulated lung fluids. *Atmos. Environ.* **2014**, *89*, 282–289. [[CrossRef](#)]
38. Jin, Y.; Yuan, C.; Jiang, W.; Qi, L. Evaluation of bioaccessible arsenic in fly ash by an in vitro method and influence of particle-size fraction on arsenic distribution. *J. Mater. Cycles Waste Manag.* **2013**, *15*, 516–521. [[CrossRef](#)]

39. Lokeshappa, B.; Dikshit, A.K.; Luo, Y.; Hutchinson, T.J.; Giammar, D.E. Assessing bioaccessible fractions of arsenic, chromium, lead, selenium and zinc in coal fly ashes. *Int. J. Environ. Sci. Technol.* **2014**, *11*, 1601–1610. [[CrossRef](#)]
40. Bourliva, A.; Papadopoulou, L.; Aidona, E.; Simeonidis, K.; Vourlias, G.; Devlin, E.; Sanakis, Y. Enrichment and oral bioaccessibility of selected trace elements in fly ash-derived magnetic components. *Environ. Sci. Pollut. Res.* **2017**, *24*, 2337–2349. [[CrossRef](#)]
41. Bourliva, A.; Papadopoulou, L.; da Silva, E.F.; Patinha, C. In vitro assessment of oral and respiratory bioaccessibility of trace elements of environmental concern in Greek fly ashes: Assessing health risk via ingestion and inhalation. *Sci. Total Environ.* **2020**, *704*, 135324. [[CrossRef](#)]
42. Ruby, M.V.; Davis, A.; Schoof, R.; Eberle, S.; Sellstone, C.M. Estimation of lead and arsenic bioavailability using a physiologically based extraction test. *Environ. Sci. Technol.* **1996**, *30*, 422–430. [[CrossRef](#)]
43. Denys, S.; Caboche, J.; Tack, K.; Rychen, G.; Wragg, J. In vivo validation of the unified BARGE method to assess the bioaccessibility of arsenic, antimony, cadmium, and lead in soils. *Environ. Sci. Technol.* **2012**, *46*, 6252–6260. [[CrossRef](#)]
44. ISO 17924; Soil Quality—Assessment of Human Exposure from Ingestion of Soil and Soil Material—Procedure for the Estimation of the Human Bioaccessibility/Bioavailability of Metals in Soil. ISO: Genève, Switzerland, 2018.
45. Pelfrène, A.; Cave, M.R.; Wragg, J.; Douay, F. In vitro investigations of human bioaccessibility from reference materials using simulated lung fluids. *Int. J. Environ. Res. Public Health* **2017**, *14*, 112. [[CrossRef](#)] [[PubMed](#)]
46. Wragg, J.; Cave, M.; Basta, N.; Brandon, E.; Casteel, S. An inter-laboratory trial of the unified BARGE bioaccessibility method for arsenic, cadmium and lead in soil. *Sci. Total Environ.* **2011**, *409*, 4016–4030. [[CrossRef](#)] [[PubMed](#)]
47. Hamilton, E.M.; Barlow, T.S.; Gowing, C.J.B.; Watts, M.J. Bioaccessibility performance data for fifty-seven elements in guidance material BGS 102. *Microchem. J.* **2015**, *123*, 131–138. [[CrossRef](#)]
48. Silva, L.F.O.; DaBoit, K.; Sampaio, C.H.; Jasper, A.; Andrade, M.L.; Kostova, I.J.; Waanders, F.B.; Henke, K.R.; Hower, J.C. The occurrence of hazardous volatile elements and nanoparticles in Bulgarian coal fly ashes and the effect on human health exposure. *Sci. Total Environ.* **2012**, *416*, 513–526. [[CrossRef](#)] [[PubMed](#)]
49. Vassilev, S.V.; Menendez, R.; Alvarez, D.; Dias-Somoano, M.; Martinez-Tarazona, R.M. Phase-mineral and chemical composition of coal fly ashes as a basis for their multicomponent utilization. 1. Characterization of feed coals and fly ashes. *Fuel* **2003**, *82*, 1793–1811. [[CrossRef](#)]
50. Yang, J.; Zhao, Y.; Zyryanov, V.; Zhang, J.; Zheng, C. Physical–chemical characteristics and elements enrichment of magnetospheres from coal fly ashes. *Fuel* **2014**, *135*, 15–26. [[CrossRef](#)]
51. Cui, J.-L.; Zhao, Y.-P.; Li, J.-S.; Beiyuan, J.-Z.; Tsang, D.C.W.; Poon, C.-S.; Chan, T.-S.; Wang, W.-X.; Li, X.-D. Speciation, mobilization, and bioaccessibility of arsenic in geogenic soil profile from Hong Kong. *Environ. Pollut.* **2018**, *223*, 375–384. [[CrossRef](#)]
52. Fu, B.; Hower, J.C.; Li, S.; Huang, Y.; Zhang, Y.; Hu, H.; Liu, H.; Zhou, J.; Zhang, S.; Liu, J.; et al. The key roles of Fe-bearing minerals on arsenic capture and speciation transformation during high-As bituminous coal combustion: Experimental and theoretical investigations. *J. Hazard. Mater.* **2021**, *415*, 125610. [[CrossRef](#)]
53. Palumbo-Roe, B.; Wragg, J.; Cave, M. Linking selective chemical extraction of iron oxyhydroxides to arsenic bioaccessibility in soil. *Environ. Pollut.* **2015**, *207*, 256–265. [[CrossRef](#)]
54. Kelepertzis, E.; Chastný, V.; Botsou, F.; Sigala, E.; Kypridou, Z.; Komárek, M.; Skordas, K.; Argyraki, A. Tracing the sources of bioaccessible metal(loid)s in urban environments: A multidisciplinary approach. *Sci. Total Environ.* **2021**, *771*, 144827. [[CrossRef](#)]
55. Morais, M.A.; Gasparon, M.; Delbem, I.D.; Caldeira, C.L.; Freitas, E.T.F.; Ng, J.C.; Ciminelli, V.S.T. Gastric/lung bioaccessibility and identification of arsenic-bearing phases and sources of fine surface dust in a gold mining district. *Sci. Total Environ.* **2019**, *689*, 1244–1254. [[CrossRef](#)] [[PubMed](#)]

Disclaimer/Publisher’s Note: The statements, opinions and data contained in all publications are solely those of the individual author(s) and contributor(s) and not of MDPI and/or the editor(s). MDPI and/or the editor(s) disclaim responsibility for any injury to people or property resulting from any ideas, methods, instructions or products referred to in the content.